JOURNAL OF MATERIALS SCIENCE **38** (2003) 4293–4300

Solid-state sensors for in-line monitoring of NO_2 in automobile exhaust emission

G. M. KALE*
*Institute for Materials Research, Houldsworth Building, University of Leeds,
Leeds LS2 9JT, UK
E-mail: g.m.kale@leeds.ac.uk*

L. WANG
*Department of Materials Science and Metallurgy, University of Cambridge,
Cambridge CB2 3QZ, UK*

J. E. HAYES
*Department of Mining and Mineral Engineering, Houldsworth Building,
University of Leeds, Leeds LS2 9JT, UK*

J. CONGJIN, Y. R. HONG
*Department of Materials Science, University of Science and Technology Beijing,
Beijing 10083, People's Republic of China*

Three types of planar solid-state sensors for measuring NO_2 in a gas mixture has been designed and tested in the laboratory under controlled atmosphere between 573–723 K. The concentration of NO_2 in the gas mixture was in the range of 0–500 ppm with the balance gas consisting of air. The three types of NO_2 gas sensors that have been tested in this investigation can be schematically represented as follows:

$$\text{Pt}, NO_2 + \text{air}, NaNO_3 + Ba(NO_3)_2 \,|\, \text{NASICON disk} \,|\, \text{Porous YSZ disk} \,|\, NO_2 + \text{air}, \text{Pt} \qquad \text{(I)}$$

$$\text{Pt}, NO_2 + \text{air}, NaNO_3 + Ba(NO_3)_2 \,|\, \text{NASICON disk} \,|\, \text{YSZ thin film} \,|\, NO_2 + \text{air}, \text{Pt} \qquad \text{(II)}$$

$$\text{Pt}, NO_2 + \text{air}, \text{Pt} \,|\, \text{YSZ disk} \,|\, \text{Au} - \text{Pd},\ NO_2 + \text{air}, \text{Pt} \qquad \text{(III)}$$

In sensor (I) the two solid electrolyte disks were attached by diffusion bonding at elevated temperature whereas in sensor (II) the (8 mol% Y_2O_3–ZrO_2) YSZ thin film was deposited on ($Na_3Zr_2Si_2PO_{12}$) NASICON disk by radio frequency (RF) magnetron sputtering technique. The measured open circuit electromotive force (Emf) of each sensor was found to attain stable value at all the concentrations of NO_2 in the gas mixture and also varied linearly as a function of the logarithm of the partial pressure of NO_2 in the gas mixture. The time required to reach 90% of the stable emf at a fixed concentration of NO_2 and at a constant temperature was found to be 30–40 min for sensor (I) and approximately 2–3 min for sensor (II) and (III). © *2003 Kluwer Academic Publishers*

1. Introduction

Combustion of fossil fuels is the main source of atmospheric pollutants such as NO_X ($X = 1, 2$), SO_X ($X = 2, 3$) and CO_2. Continuous monitoring and control of atmospheric pollutants using chemical sensor will be extremely useful for a continuous process control and emission monitoring in the industries using oil fired burners, diesel engine road vehicles (DERV), petrol fuelled automobiles and also to the environmental agencies for the development of novel pollution management strategies and policies for the improvement of the quality of environment and health.

According to recent statistics, 2 million tons of NO_X was sent into the atmosphere by diesel and petrol fuelled automobiles in Germany in 1986 [1]. Similarly, about 70% of the 2.06 million tons of NO_X emitted in the UK in 1996 was produced by automobiles and power generating industries [2]. In order to control the ever increasing emission of NO_X by fuel combustion, it is necessary to design more efficient processes and more greener power generation technologies. In order to achieve this it is necessary to design reliable and robust chemical sensors for in-line monitoring of the emissions from combustion processes.

---

* Author to whom all correspondence should be addressed.

Several types of NO_X sensors such as the resistive or conductive type sensors using semiconductors [3–5] or metal phthalocyanines [6], and electrochemical sensors using solid electrolytes [7–17] have been investigated by different research groups in various parts of the world. Among the various types of NO_X sensors, the electrochemical sensors using solid electrolytes are of high sensitivity, high selectivity and simple construction, so these sensors are promising. Gauthier and Chamberland [7] have reported that a solid electrolyte sensor using $Ba(NO_3)_2 + 1\%AgCl$ could respond to NO_2 (5–500 ppm in air) at 754 K. Recently, NO_X sensors combining β/β''-alumina and nasicon with $NaNO_3$ or $NaNO_2$ were reported to operate at around 423–523 K [8, 12, 16]. Based on these investigations it can be inferred that the choice of the auxiliary electrode materials and design of the sensor are important factors for a reliable sensor response. For example, NO_2 sensing characteristics can be much improved by the use of an auxiliary electrode made from a binary salt system such as $NaNO_3$—$Ba(NO_3)_2$, $NaNO_2$—Li_2CO_3 and $NaNO_2$—Na_2CO_3, and the device using $NaNO_2$—Li_2CO_3 [12] has an ability to detect NO_2 concentrations as low as ppb level in air between 423–523 K. However, there are structural issues such as size, geometry i.e., planar or tube type, porous or fully dense electrode and/or electrolyte, etc, issues related to the chemical stability of electrodes, electrolytes and auxiliary electrode material, response time and stability of the sensor signal in testing environments that need to be carefully looked into for successfully developing a practical NO_X sensors. In order to understand the effect of some of the issues on response time and stability of sensor signal, we have tested three different types of planar sensors for measuring NO_2 in a gas mixture synthesised in a laboratory environment. The sensors can be represented schematically as follows:

$$\begin{aligned}&\text{Pt, } NO_2 + \text{air, } NaNO_3 + Ba(NO_3)_2 \mid \text{Nasicon disk}\\ &\quad \mid \text{Porous YSZ disk} \mid NO_2 + \text{air, Pt} \qquad \text{(I)}\end{aligned}$$

$$\begin{aligned}&\text{Pt, } NO_2 + \text{air, } NaNO_3 + Ba(NO_3)_2 \mid \text{Nasicon disk}\\ &\quad \mid \text{YSZ thin film} \mid NO_2 + \text{air, Pt} \qquad \text{(II)}\end{aligned}$$

$$\text{Pt, } NO_2 + \text{air, Pt} \mid \text{YSZ disk} \mid \text{Au-Pd, } NO_2 + \text{air, Pt} \qquad \text{(III)}$$

2. Experimental

2.1. Materials and sensor fabrication

Fine powder of $Na_3Zr_2Si_2PO_{12}$ (nasicon) solid electrolyte was prepared by direct solid-state reaction [18, 19]. High purity fine powders of anhydrous sodium carbonate (Na_2CO_3), zirconium dioxide (ZrO_2), silicon dioxide (SiO_2) and ammonium di-hydrogen phosphate ($NH_4H_2PO_4$) obtained from Aldrich Chemical Co. (UK) were used as starting materials. They were weighed according to the required molar ratio and ground in a zirconia ball mill under acetone. The slurry was dried between 330 to 350 K for 6 h, calcined at 483 K for 5 h to decompose $NH_4H_2PO_4$, and further calcined at 1173 K for 6 h to decompose Na_2CO_3 in ambient atmosphere. Two stage calcinations were found to be essential to give enough time for the binary oxides to react and form single phase $Na_3Zr_2Si_2PO_{12}$. Formation of a single phase Nasicon was confirmed by X-ray diffraction (XRD) procedure using Cu K_α as a radiation and the XRD pattern of single phase $Na_3Zr_2Si_2PO_{12}$ is shown in Fig. 1. After the final calcination step, the mixture was ball milled again to produce fine powders of Nasicon in the range of 5–10 μm.

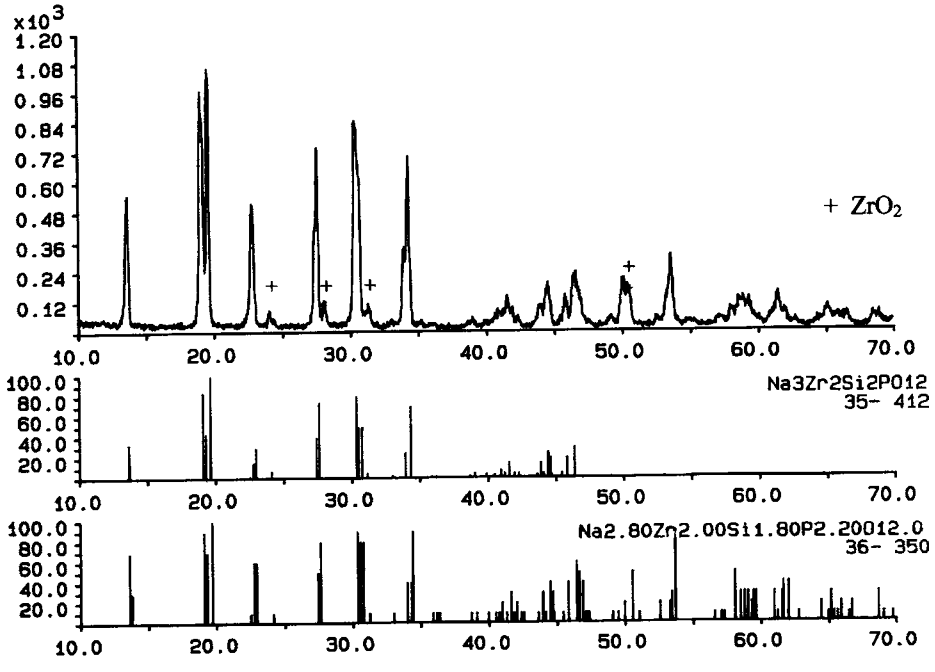

Figure 1 Comparison of the X-ray diffraction pattern of $Na_3Zr_2Si_2PO_{12}$ with a nearest match available in JCPDS.

The solid electrolyte couple for sensor (I) was made by isostatically compacting approximately 1.5 mm thick layers of Nasicon and YSZ powders together in a soft polymeric mould at 400 MPa. The bilayered powder compact was sintered at 1503 K for 4 h as described earlier [18] resulting into a dense Nasicon disk that was diffusion bonded to YSZ disk. Platinum electrodes were coated on the outer surface of the bi-electrolyte couple by sputtering technique using high purity Pt-target at ambient temperature. The assembly was subsequently cured at 1123 K for 60 min in order to improve adhesion of platinum electrode to the ceramic electrolyte surface. The sensing electrode of the sensor (I) consisting of $Ba(NO_3)_2$—$NaNO_3$ eutectic powder in 4:1 ratio was mixed with an organic liquid binder and coated on the Nasicon surface of the bielectrolyte compact using a paint brush.

The solid electrolyte couple for sensor (II) was made as follows. The Nasicon powder was isostatically pressed into pellets of 10 mm in diameter and 1 mm thick at a pressure of 400 MPa and then sintered at 1503 K for 4 h in air inside a platinum crucible covered with a platinum lid to prevent any change in composition of Nasicon pellet as a result of volatilisation of Na_2O at elevated temperature during sintering. The temperature of the furnace was ramped at the rate of 3 K min^{-1} while heating and cooling. The sintered pellet of Nasicon was polished in stages down to 1 μm surface finish in a water free medium in order to prevent hydration of the surface of Nasicon pellet during polishing and washed with absolute alcohol. A thin film of (8 mol% Y_2O_3)-ZrO_2 (YSZ) approximately 6 μm thick was deposited on one of the polished surface of Nasicon pellet by multiple radio frequency (RF) magnetron sputtering [20] using US Gun II (Film Product Company, USA) equipment. During the RF sputtering of YSZ powder, obtained from Tosho Co. (Japan), on Nasicon pellet the working gas was 99% pure argon, gas pressure was 0.67 Pa, RF power was 300 W, substrate temperature was maintained at 298 K and the distance between the target and Nasicon substrate was 14 cm. The Pt electrodes were coated on the two surfaces of the bielectrolyte couple as described earlier. The sensing electrode of sensor (II) consisting of $Ba(NO_3)_2$—$NaNO_3$ eutectic powder in 4:1 ratio was mixed with an organic liquid binder and coated on the Nasicon surface of the bielectrolyte compact using a paint brush.

Sensor (III) was fabricated from a 250 μm thick high density YSZ disk produced by isostatically pressing fine powder at 400 MPa followed by sintering the compact at 1823 K for 2 h. The microstructure of the sintered disk is shown in Fig. 2. The Au-Pd and Pt electrodes of sensor (III) were sputter coated using a vacuum sputtering technique in argon atmosphere at ambient temperature and a pressure of 1.33 Pa. Pt wires having 127 μm diameter were attached to the two electrodes of each type of sensor by using an Engelhardt A4731 Pt-ink.

2.2. Measurement

The emf of the three types of NO_2 sensors (I)–(III) was measured at a fixed temperature over a range of concentrations of NO_2 between 0–500 ppm using a Keithley 6517A high impedance ($\geq 10^{12}$ Ω) multi-channel digital electrometer. The gas mixture of NO_2 and air with different NO_2 concentrations was prepared by mixing air and 500 ppm NO_2 + air using computer controlled mass-flow controllers. A total flow rate of measuring gas was maintained at 100 cm^3 min^{-1}. Sufficient care was taken to convert any NO present in the gas mixture into NO_2 by passing over a granular catalyst supported on alumina spheres of approximately 1–2 mm diameter. The response of the sensor at a fixed temperature was recorded on a personal computer using a commercial software provided by Keithley Instruments. A schematic diagram of the experimental set-up is presented in Fig. 3.

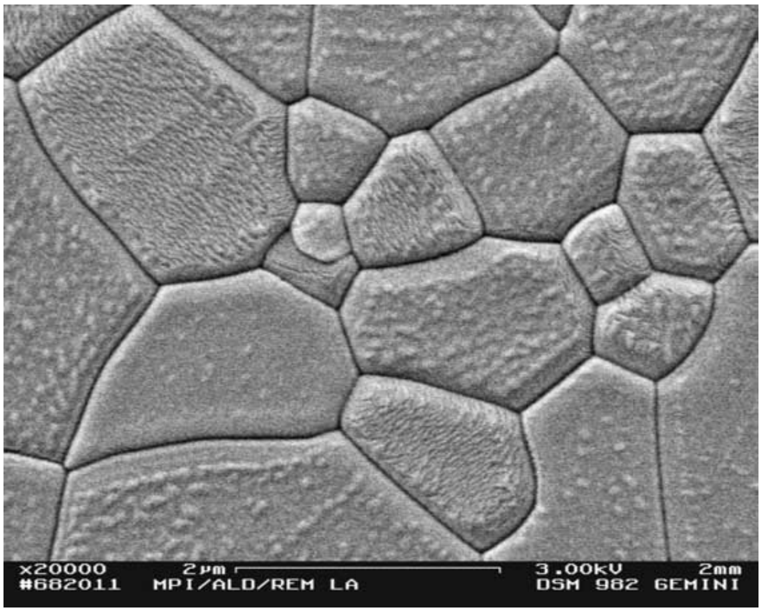

Figure 2 Microstructure of sintered (8 mol%Y_2O_3) ZrO_2.

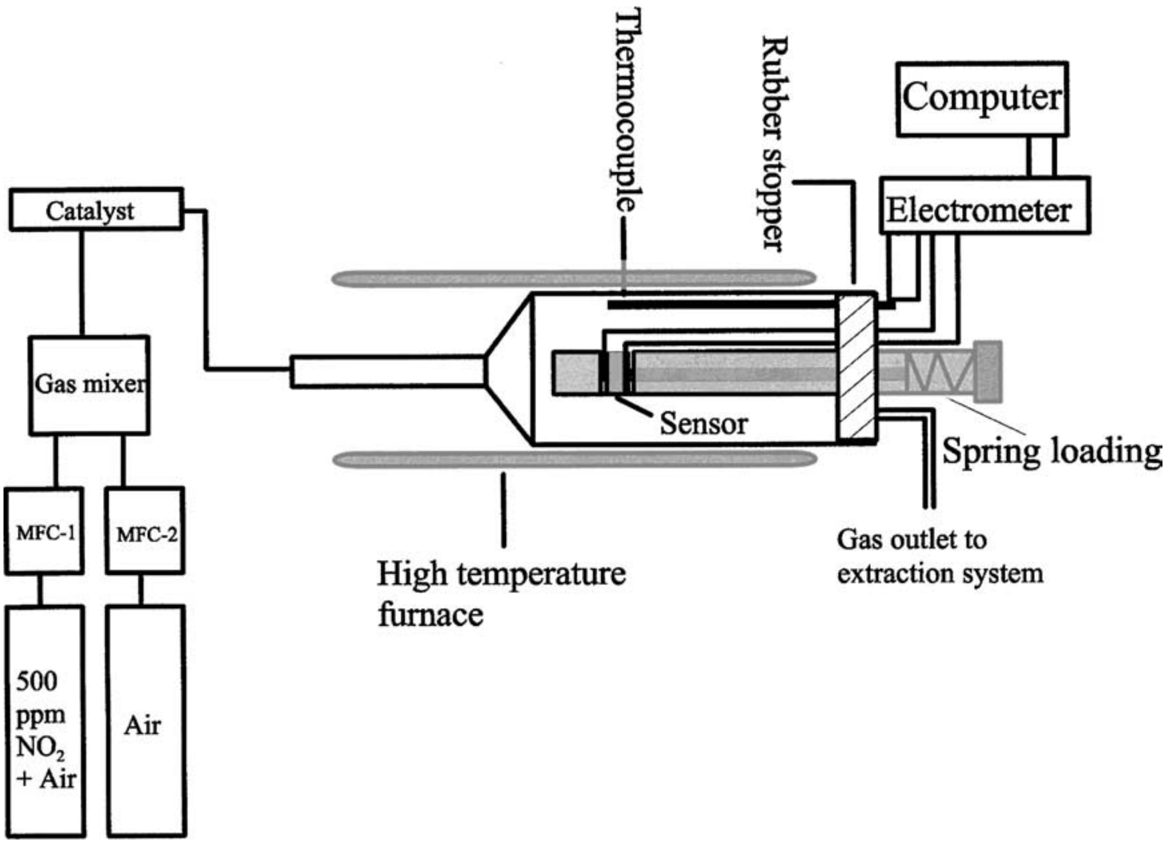

Figure 3 Schematic diagram of the gas sensor testing apparatus.

3. Results and discussion

Sensor (I) was tested at 573 K between 0 and 500 ppm of NO_2. The response of sensor (I) at 573 K is shown in Fig. 4. The noise in the measured signal was found to be less than 1% of the value of the open circuit emf at any given time during the measurements. The 90% of the stable value of the emf was reached within 30 min after the change of concentration of NO_2 in the gas mixture however for the concentrations of NO_2 between 250 ppm and 500 ppm the time required for attaining 90% of the stable emf value was around 40 min. It can be seen in Fig. 4 that sensor (I) responded to change in concentration of NO_2 almost instantaneously and the emf of the sensor was found to be stable up to 1000 min. The measured emf of sensor (I) was found to vary linearly as a function of the concentration of NO_2 in the gas mixture at 573 K as shown in Fig. 5. It is believed that the sensing mechanism of sensor (I) can be described according to the following set of electrode or interfacial reactions [18, 21]. At the sensing electrode

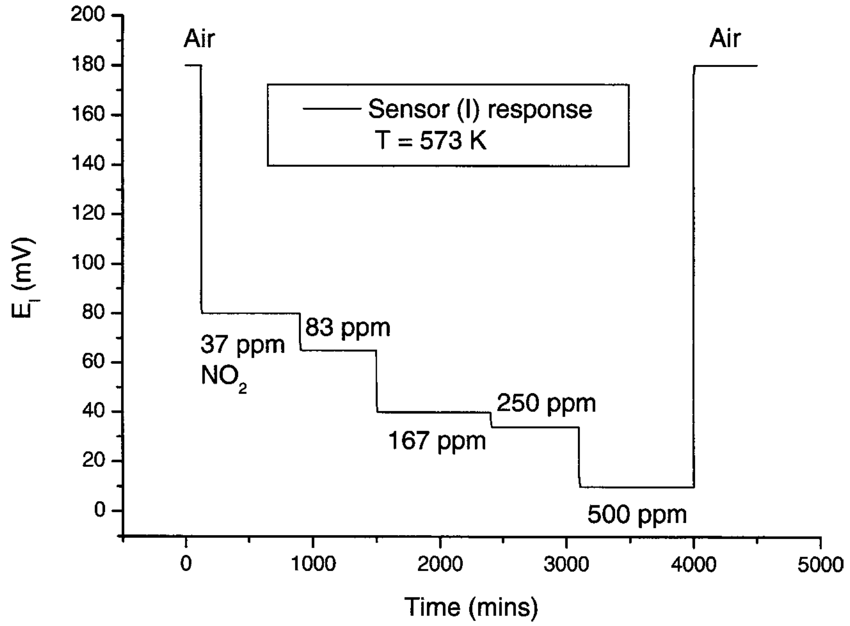

Figure 4 Response of sensor (I) to change in concentration of NO_2 in the gas mixture.

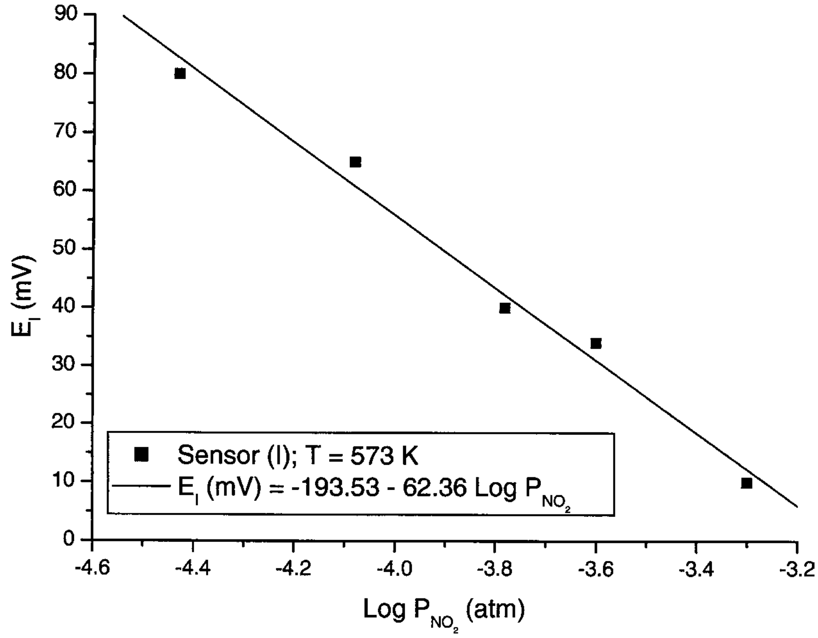

Figure 5 Variation of the emf of sensor (I) as a function of NO_2 concentration.

consisting of $Ba(NO_3)_2 + NaNO_3$,

$$2NaNO_3\,(s) \rightarrow 2Na^+ + 2NO_2\,(g) + O_2\,(g) + 2e^- \qquad (1)$$

The following reaction occurs at the YSZ electrode,

$$\frac{1}{2}O_2\,(g) + 2e^- \rightarrow O^{2-} \qquad (2)$$

At the interface between the Nasicon and YSZ electrolyte,

$$2Na^+ + O^{2-} \rightarrow Na_2O\,(s)_{\text{Nasicon}} \qquad (3)$$

The net cell reaction is,

$$2NaNO_3\,(s) \rightarrow Na_2O\,(s)_{\text{Nasicon}} + 2NO_2\,(g) + \frac{1}{2}O_2\,(g) \qquad (4)$$

At a fixed temperature of measurement and, for a fixed composition of the sensing electrode and Nasicon solid solution the emf of sensor (I) in which the gas composition at the two electrodes is identical will be dependent only on the concentration of NO_2 in the gas mixture. Therefore, it can be easily shown that the emf of sensor (I) can be given by the following expression [21]:

$$E\,(\text{mV}) = E^\circ - 0.1T\,\text{Log}\,P_{NO_2} \qquad (5)$$

In Equation 5, E° is a constant determined by the factors such as the activity of Na_2O in Nasicon, activity of $NaNO_3$ in the sensing electrode, standard Gibbs' energy change for Reaction 4, temperature of measurement, the universal gas constant, the Faraday constant and the number electrons participating in the electrode reactions. From Equation 5 it can be inferred that at a constant temperature the measured open circuit voltage of NO_2 sensor (I) should vary linearly as a function of the partial pressure of NO_2 in the gas mixture and the slope of the linear segment should be equal to $0.1T$, where T is the temperature in Kelvin. The variation of the measured emf of sensor (I) as a function of the partial pressure of NO_2 in the gas mixture at 573 K is shown in Fig. 5. The least squares regression analysis of the data presented in Fig. 5 gives,

$$E_I\,(\text{mV}) = -193.53 - 62.36\,\text{Log}\,P_{NO_2}(\pm 10) \qquad (6)$$

The slope of the linear segment given by Equation 6 is in good agreement with the theoretical value of 57.3 for a two-electron process.

Similar measurements were carried out on sensor (II) in a gas mixture containing NO_2 at 673 K and at 723 K. A typical response of the sensor (II) at 723 K is shown in Fig. 6a and b and similar response was obtained at 673 K too. Sensor (II) was found to respond more rapidly to change in concentration of NO_2 in the gas mixture compared to sensor (I). The noise in the measured signal was found to be less than 1% of the value of the open circuit emf at any given time during the measurements. The sensor was found to reach 90% of the stable value of the open circuit emf at a fixed NO_2 concentration and at a fixed temperature in less than 2 min. This may be due to the considerable reduction of the diffusion distance because of the use of a thin film of YSZ in sensor (II) compared to a thick porous disk in sensor (I) suggesting that the thin film sensor would respond more rapidly compared to a thick film sensor. It can be seen in Fig. 6a that the sensor (II) responded instantly to change in concentration of NO_2 in the gas mixture from nought to 90 ppm whereas the recovery of the sensor to the original emf in air was slightly sluggish. This is probably due to the slow rate of removal of NO_2 from the sensor testing apparatus after cutting off the supply of NO_2 to the sensor (II). The response of sensor (II) to the change in concentration of NO_2 in the gas mixture was found to be considerably rapid when the concentration of NO_2 in the gas mixture was changed from 450 ppm down to 90 ppm and back up to 450 ppm as seen in Fig. 6b. The variation of the

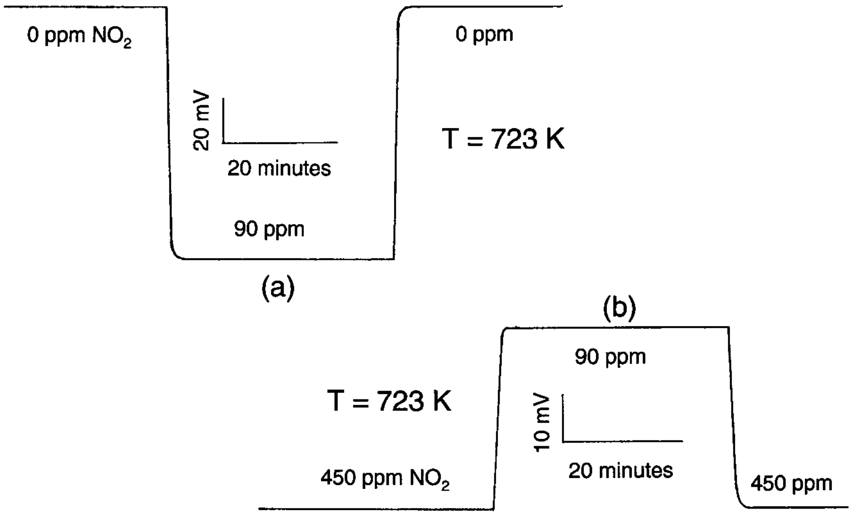

Figure 6 Response of sensor (II) to change in NO_2 concentration.

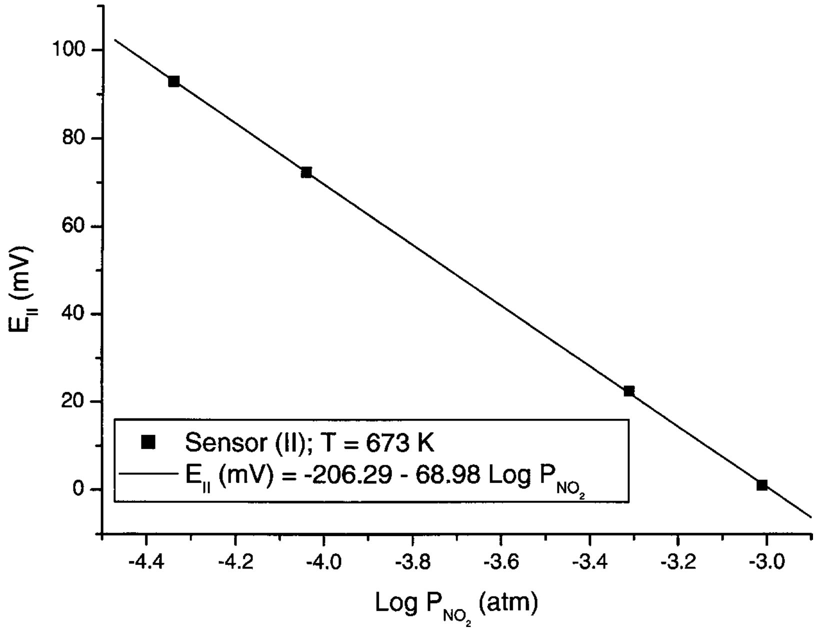

Figure 7 Measured emf of sensor (II) as a function of NO_2 concentration at 673 K.

measured emf of sensor (II) as a function of the concentration of NO_2 in the gas mixture at 673 K and 723 K is shown in Figs 7 and 8 respectively. A least squares regression analysis of the measured emf of sensor (II) at 673 K and at 723 K, respectively, gives,

$$E_{\text{II}}\,(\text{mV}) = -206.29 - 68.98\,\text{Log}\,P_{NO_2}\,(\pm 10) \quad (7)$$

$$E_{\text{II}}\,(\text{mV}) = -268.57 - 76.21\,\text{Log}\,P_{NO_2}\,(\pm 10) \quad (8)$$

The slope of the linear segments shown in Figs 7 and in 8 are in excellent agreement with the theoretical values, 67.3 and 72.3, calculated using Equation 5.

Sensor (III) was tested at 688 K in a flowing gas mixture consisting of air and varying concentrations of NO_2. A typical response of the sensor (III) to change in concentration of NO_2 in the gas mixture is shown in Fig. 9. The noise in the measured signal was found to be less than 1% of the value of the open circuit emf at any given time during the measurements. Sensor (III) was found to respond almost instantly to changes in the concentration of NO_2 in the gas mixture. The sensor was found to reach a 90% of the stable value of the open circuit emf at a fixed temperature and concentration of NO_2 within 2 min. Again the rapid response of sensor (III) compared to sensor (I) is probably due to the use of 250 micrometer high density disk of YSZ instead of a sintered pellet. The behaviour of sensor (III) can be explained based on the mixed potential generated as a result of the following electrode reactions [22],

$$NO_2\,(g) + 2e^- \rightarrow NO\,(g) + O^{2-} \quad (9)$$

$$O^{2-} \rightarrow \frac{1}{2}O_2\,(g) + 2e^- \quad (10)$$

The variation of the measured emf of sensor (III) as a function of the concentration of NO_2 in the gas mixture is shown in Fig. 10. Least squares regression analysis

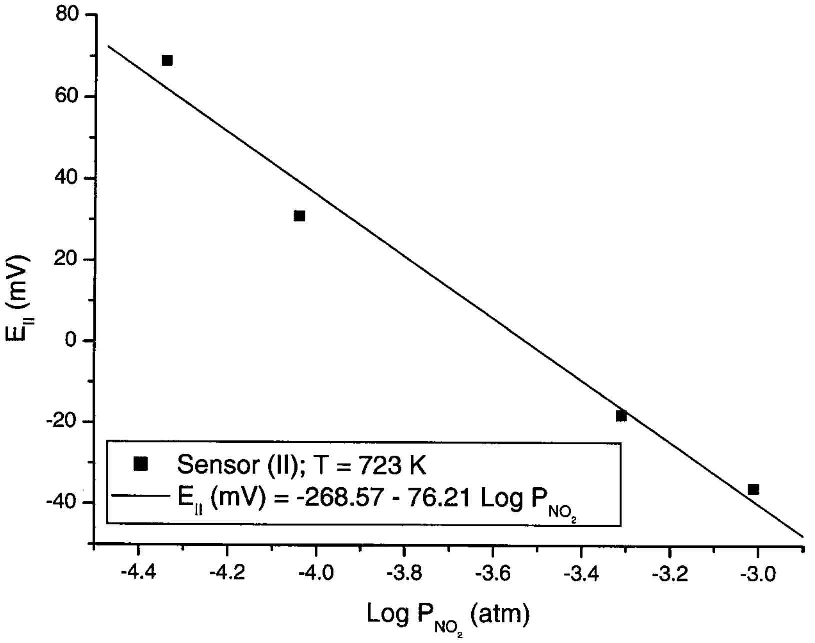

Figure 8 Measured emf of sensor (II) as a function of NO_2 concentration at 723 K.

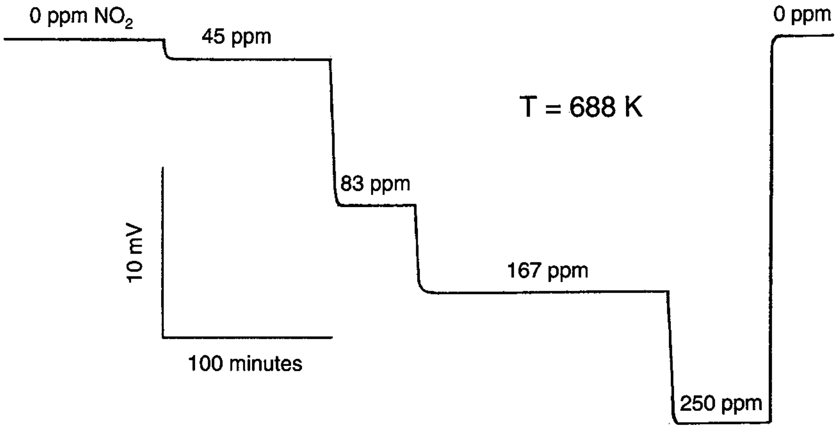

Figure 9 Response of sensor (III) to change in concentration of NO_2 concentration.

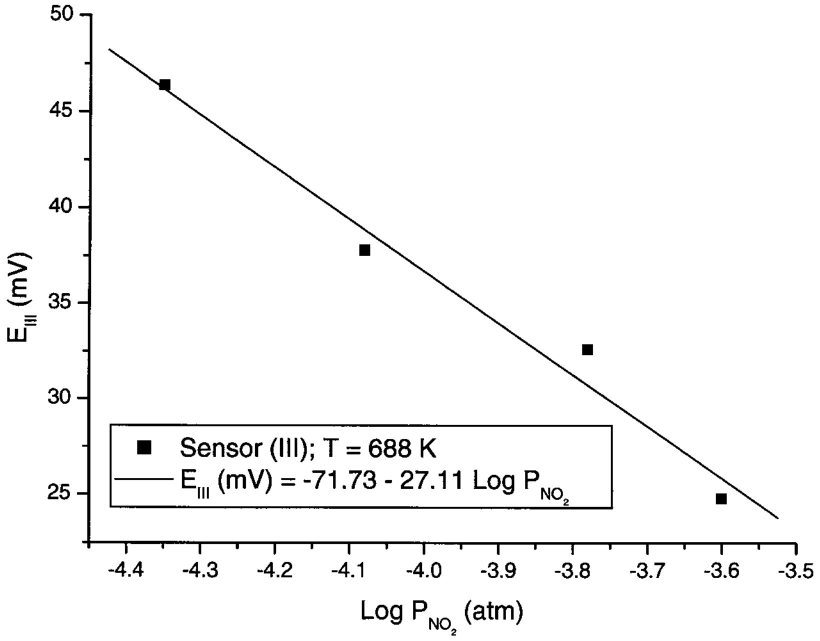

Figure 10 Variation of the emf of sensor (III) as a function of NO_2 concentration.

of the data gives,

$$E_{\mathrm{III}}\,(\mathrm{mV}) = -71.73 - 27.11\,\mathrm{Log}\,P_{\mathrm{NO_2}}(\pm 10) \quad (11)$$

This clearly suggests that the measured emf of sensor (III) varies linearly as a function of the concentration of NO_2 in the gas mixture.

4. Conclusions

Three types of sensors, two potentiometric sensors based on a bi-electrolyte couple and a mixed potential sensor based on oxide ion-conducting ceramic membrane have been successfully fabricated and tested in air + NO_2 gas mixture to determine their sensing behaviour for NO_2 in the gas mixture at different temperatures. All the three types of planar sensors have been found to respond instantly to the change in NO_2 concentration in the gas mixture however the response of sensor (II) and (III) was found to be significantly rapid (2–3 min) compared to that of sensor (I) (30–40 min). This may be due to significantly small diffusion distance for mobile ions in the solid electrolytes of sensor (II) and (III) compared to sensor (I). Therefore, it can be concluded that a thin film sensor is likely to respond more rapidly compared to a thick film sensor. The measured emf of each sensor was found to vary linearly as a function of the logarithm of NO_2 concentration in the gas mixture. In order to use this type of sensors in the automobile exhaust system, we plan to investigate the response of the NO_2 sensors in the gas mixtures containing other gases that are usually present in the automobile exhaust emissions.

Acknowledgement

Authors wish to express their gratitude to The Royal Society (UK), Institution of Materials, Minerals and Mining (UK) and National Natural Science Foundation of China for supporting the sensors research. GMK wishes to acknowledge the support of Max-Planck Foundation for the electron microscopy work at the Max-Planck Institute fur Metallforschung in Stuttgart (Germany).

References

1. H. MEIXNER, J. GERBLINGER, V. LAMPE and FLEISCHER, *Sensors and Actuators* B **23** (1995) 119.
2. A. G. SALWAY, H. S. EGGLESTON, J. W. L. GOODWIN, J. E. BERRY and T. P. MURRELLS, "UK Emissions of Air Pollutants" (Department of the Environment, Transport and the Regions, London, 1999) p. 43.
3. G. SBERVEGLIERI, S. GROPPELLI, P. NELLI, V. LANTO and H. TORVELA, *Sensors and Actuators* **B1** (1990) 79.
4. T. ISHIHARA, K. SHIOKAWA, K. EGUCHI and H. ARAI, *ibid.* **19** (1989) 259.
5. M. AKIYAMA, J. TAMAKI, N. MIURA and N. YAMAZOE, *Chem. Letts.* **1** (1991) 1611.
6. T. A. JONES, B. BOTT and S. C. THORPE, *Sensors and Actuators* **17** (1995) 467.
7. M. GAUTHIER and A. CHAMERLAND, *J. Electrochem. Soc.* **124** (1977) 1579.
8. G. HOTZEL and W. WEPPNER, *Sensors and Actuators* B **12** (1987) 449.
9. S. YAO, Y. SHIMIZU and N. YAMAZOE, *Denki Kagaku* **7** (1993) 903.
10. N. MIURA, S. YAO, Y. SHIMIZU and N. YAMAZOE, *Sensors and Actuators* B **13** (1993) 387.
11. Y. SHIMIZU, Y. OKAMOTO, S. YAO, N. MIURA and N. YAMAZOE, *Denki Kagaku* **6** (1991) 465.
12. S. YAO, Y. SHIMIZU, N. MIURA and N. YAMAZOE, *Chem. Letts.* **2** (1992) 587.
13. N. MIURA, S. YAO, Y. SHIMIZU, N. MIURA and N. YAMAZOE, *Solid State Ionics* **70/71** (1994) 572.
14. H. KUROSAWA, Y. YAN, N. MIURA and N. YAMAZOE, *ibid.* **79** (1995) 338.
15. P. THAMBOON, S. YAO, P. GOUMA and S. A. AKBAR, "Electrochemistry of Glass and Ceramics" (The American Ceramics Society Inc., Westerville, 1998) p. 221.
16. N. YAMAZOE and N. MIURA, *Mater. Res. Soc. Bull.* **24** (1999) 37.
17. N. MIURA, G. LU, N. YAMAZOE, H. KUROSAWA and M. HASEI, *J. Electrochem. Soc.* **143** (1996) L33.
18. G. M. KALE and K. T. JACOB, *J. Mater. Res.* **4** (1989) 417.
19. W. L. WORRELL, *J. Electroanal. Chem.* **168** (1984) 355.
20. L. WANG, Y. R. HONG and G. M. KALE, Unpublished research (2000).
21. G. M. KALE, A. J. DAVIDSON and D. J. FRAY, *Solid State Ionics* **86–88** (1996) 1107.
22. G. LU, N. MIURA and N. YAMAZOE, *J. Mater. Chem.* **7** (1997) 1445.

Received 4 April
and accepted 1 August 2003